

Numerical Simulations of Air Flow inside Large Refrigeration Stores Onboard Marine Ships

Amr F. Sharafeldin^{*}, Wael M. El-Maghlany^{**}, Abdelhamid Attia^{**} and Yehia A. Eldrainy^{***}

Keywords: Numerical simulation, temperature and relative humidity distribution, special stores, marine ships, large refrigeration stores, vegetables fruit storing.

20% fresh air admits acceptable internal air quality inside large refrigeration stores.

ABSTRACT

This paper aims to develop and implement a static modeling for large refrigeration stores on board marine ships. It is required several numbers of monitoring points for estimating average conditions of air quality in large stores. The simulation of temperature and relative humidity distribution inside the special stores enables the operators to predict temperature and relative humidity. Also it is an attempt to evaluate internal air quality of large refrigeration stores on board marine ships to keep internal air quality at such a condition of (1-4) °C and (70-75) % relative humidity. These represent the optimum conditions for the storage of fresh fruits and vegetables. Controlling inlet air moisture content is accomplished according to the nature of transferred product. As for simulation modeling, different models were adopted and expanded by Ansys Fluent 17.2 program. Some simulated results were validated by measurements with good agreement where a case study was conducted in a large proofer in Cairo, Egypt. A number of different models on the entrance air speeds and flow rates in large refrigeration stores were introduced. Optimum sensor locations inside the large refrigeration store were selected according to simulation results. The results showed that in order to maintain optimum large refrigeration store conditions inlet air flow rates from 3.8 m³/s to 5.2 m³/s. This air flow rate range with

Paper Received January, 2023. Revised March, 2023, Accepted May, 2023, Author for Correspondence: Amr F. Sharafeldin .

** Instructor, Mechanical Engineering Department, Faculty of Engineering, Alexandria University, Alexandria – Egypt 21544, ROC.*

*** Professor, Mechanical Engineering Department, Faculty of Engineering, Alexandria University, Alexandria – Egypt 21544, ROC.*

**** Professor, Mechanical Engineering Department, Arab Academy for Science, Technology and Maritime Transport– Egypt 21913, ROC.*

INTRODUCTION

Refrigeration slows down the chemical and biological processes in foods, and deterioration and loss of quality and nutrients. A temperature of 4C or lower is considered to be a safe refrigeration temperature. Sometimes a small increase in refrigeration temperature may cause a large increase in the growth rate, and a considerable decrease in shelf-life of the food. The loss of moisture from fresh fruits and vegetables is also called transpiration. The amount of moisture lost from a fruit or vegetable per unit mass of the fruit or vegetable per unit time is called the transpiration rate. The transpiration rate varies with the environmental conditions such as the temperature, relative humidity, and air velocity. Moisture loss can be minimized by (1) keeping the storage temperature of food as low as possible, (2) keeping the relative humidity of the storage room as high as possible, and (3) avoiding high air velocities (Bamodu et al, 2017). PĂUNESCU et al. presented a verified temperature control simulation in a warehouse for fruits and vegetables with taking into account the disruptive elements which influences its constant maintenance. Keeping a constant temperature inside the warehouse cells assures the increase of storage duration but also maintaining fruits and vegetables water, vitamins and valuable content. Samuel et al. presented basic concept and principle, methods of evaporative cooling and their application for the preservation of fruits and vegetables and economy. Zero energy cooling system could be used effectively for short-duration storage of fruits and vegetables even in hilly region. It not only reduces the storage temperature but also increases the relative humidity of the storage which is essential for maintaining the Freshness of the commodities. Trčka, et al. presented an overview of heating, ventilation and air conditioning (HVAC) system modeling and simulation. The study summarized the current approaches used for modeling HVAC components, HVAC control and HVAC systems in general. Homod (2010) demonstrated types of the

HVAC model and the advantages and disadvantages of the application of each one of them. It found out that the gray-box type is the best one to represent indoor thermal comfort. However, its application fails at the integration method where its response deviates to unreal behavior. Cinzia et al. used a CFD model simulation to support the experimental investigations, temperature fields, and local thermal comfort sensation in a nonresidential environment by only setting the external weather conditions and considering natural convection and the solar radiation influence. Popovici simulated HVAC system functionality using ANSYS-Fluent software. This type of analysis can be used for pre-examination of the future projects to obtain functional systems and verify all the requirements for the HVAC installation. Mahu et al. modeled and simulated a heating, ventilation and air conditioning (HVAC) system consisting of a simplified building with one room considering both the internal and external conditions. Amodu et al. carried out a numerical simulation using CFD to compare the air distribution of a 4-way cassette air conditioning unit with a traditional wall-mounted unit. Mengjie et al. conducted a comprehensive review of reinforcement learning (RL) techniques applied in control systems for occupant comfort in indoor built environments. Wang et al. proposed a ventilation strategy based on occupancy profiles, and captured by a Wi-Fi probe, that enabled occupancy sensing system. Based on the detected occupancy profiles, the proposed ventilation strategy and other two conventional strategies were compared in a two-day experiment conducted in a multi-zone space. Riederer presented models that are currently used for control studies and are very simplified. They consider the room's air as perfectly mixed. From this analysis, a detailed list of criteria for the development of zone models is obtained. The proposed model is able to distinguish between center air and different sensor air temperatures with time variation. Knabe et al. introduced building a simulation that considers thermal and moisture behaviors of the perimeter walls. The control of this system depends on the temperature and relative humidity that float freely in the conditioned zone. Its results are in very good agreement with the humidity response function. Kono developed a method for the modeling of in-room temperature distribution. his modeling is based on a standard two-dimensional heat diffusion equation with an effective diffusion coefficient which is identified from the characteristics of air flow inside a room and its architectural design. The effectiveness is demonstrated by comparing numerical simulations of the equation with measured data on temperature. Homod et al. investigated a hybrid PID cascade control in the central air-conditioning system in order to acquire better performance compared to the traditional PID. The simulations have found that the proposed hybrid PID-cascade controller has the capability of

self-adapting to system changes and results in faster response and better performance. Pascual et al. presented a library of simplified, physical models of different components that can be found in a typical air handling unit. The model library was developed to reduce the initial data needed for setting up a simulation model to its minimum. The main objective of this study is to investigate the effect of the inlet air speed and flow rate on large stores internal air temperature distribution, relative humidity distribution and air flow patterns in large refrigeration stores onboard marine ships. Optimum sensor locations inside the large stores were selected according to simulation results.

MATHEMATICAL MODELING

The governing equations for fluid flow

To reduce the complexity degree of solving a ventilation problem, and for the sake of completeness, the governing equations are given below in a simplified form and using tensor notation. The most significant simplification here is the approximation, which assumes that the fluid is incompressible, i.e. the variation in density is neglected. This approximation is valid for small temperature variations, which is reasonable for room air flow. The governing equations are characterized as a set of transient, coupled and nonlinear, elliptic, partial differential equations of second order.

Energy transport equation:

$$\left[\frac{\partial(ut_{xx})}{\partial x} + \frac{\partial(ut_{yx})}{\partial y} + \frac{\partial(ut_{zx})}{\partial z} + \frac{\partial(ut_{xy})}{\partial x} + \frac{\partial(ut_{yy})}{\partial y} + \frac{\partial(ut_{zy})}{\partial z} + \frac{\partial(ut_{xz})}{\partial x} + \frac{\partial(ut_{yz})}{\partial y} + \frac{\partial(ut_{zz})}{\partial z} \right] - \left(\frac{\partial(up)}{\partial x} + \frac{\partial(vp)}{\partial y} + \frac{\partial(wp)}{\partial z} \right) + \frac{\partial}{\partial x} \left(k_{eff} \frac{\partial T}{\partial x} \right) + \frac{\partial}{\partial y} \left(k_{eff} \frac{\partial T}{\partial y} \right) + \frac{\partial}{\partial z} \left(k_{eff} \frac{\partial T}{\partial z} \right) + s = 0 \quad (1)$$

Continuity equation:

$$\frac{\partial u}{\partial x} + \frac{\partial v}{\partial y} + \frac{\partial w}{\partial z} = 0 \quad (2)$$

Momentum equation (Navier-Stokes) transport equations (3 equations, for x, y, z directions):

x-direction momentum:

$$\rho \left(\frac{\partial(u^2)}{\partial x} + \frac{\partial(uv)}{\partial y} + \frac{\partial(uw)}{\partial z} \right) = -\frac{\partial p}{\partial x} + \frac{\partial}{\partial x} \left(\mu_{eff} \frac{\partial u}{\partial x} \right) + \frac{\partial}{\partial y} \left(\mu_{eff} \frac{\partial u}{\partial y} \right) + \frac{\partial}{\partial z} \left(\mu_{eff} \frac{\partial u}{\partial z} \right) \quad (3)$$

y-direction momentum:

$$\begin{aligned} \rho \left(\frac{\partial(vu)}{\partial x} + \frac{\partial(v^2)}{\partial y} + \frac{\partial(vw)}{\partial z} \right) \\ = -\frac{\partial p}{\partial y} + \frac{\partial}{\partial x} \left(\mu_{eff} \frac{\partial v}{\partial x} \right) \\ + \frac{\partial}{\partial y} \left(\mu_{eff} \frac{\partial v}{\partial y} \right) + \frac{\partial}{\partial z} \left(\mu_{eff} \frac{\partial v}{\partial z} \right) \end{aligned} \quad (4)$$

z-direction momentum

$$\begin{aligned} \rho \left(\frac{\partial(vu)}{\partial x} + \frac{\partial(v^2)}{\partial y} + \frac{\partial(vw)}{\partial z} \right) \\ = -\frac{\partial p}{\partial z} + \frac{\partial}{\partial x} \left(\mu_{eff} \frac{\partial v}{\partial x} \right) \\ + \frac{\partial}{\partial y} \left(\mu_{eff} \frac{\partial v}{\partial y} \right) + \frac{\partial}{\partial z} \left(\mu_{eff} \frac{\partial v}{\partial z} \right) \end{aligned} \quad (5)$$

Physical Domain

The CFD model was designed with much precision in geometrical configuration as the real large storing room. Product storing trays were subsequently added to the geometry. The present large storing room configuration is with main dimensions of 35 m x 9.2 m and of height 3.0 m as shown in Figure.1.

Mesh Generation

The domain meshing is created using ANSYS ICEM-CFD. The generated mesh resolution is varied so that the high-density meshing is concentrated in

Boundary conditions

For this study, the boundary conditions were defined as follows:

Table 1: Boundary Conditions

No.	Boundary Condition	Description and values
1	Internal Walls	A no-slip shear condition was selected. The wall heat flux was calculated 15w/m ² . The thermal resistance was set at 7.103 k/w, and the heat-transfer coefficient was set at 0.15w/m ² k.
2	External walls	A no-slip shear condition was selected. The wall heat flux was 32w/m ² .
3	Ceiling	A no-slip shear condition was selected. The ceiling heat flux was 17w/m ² .
4	Velocity inlet	The inlet temperature was set at T _{db} 0°C, T _{wb} -1.2°C. Inlet relative humidity 80%. The hydraulic diameter of the inlet duct was 0.1 m. The turbulence intensity was set at 5%.
5	Pressure outlet	Gauge pressure 0 Pascal. Back flow temperature 4°C

Modeling validation

For the purpose of numerical model validation, real site measurements were done in a large proofing room in the food factory of Egyptian Belgian for Industrial Investments Company at Abo Rawash, Cairo, Egypt. Some simulated results were validated by measurements with good agreement Total 70 points at the midsection of the room 1.5 m above floor level were selected for measurement of air

the high gradient zone i.e. adjacent to the dough surface and in the boundary zones. Because of the complex computation domain geometry, all mesh is unstructured mesh with maximum skewness of 0.63. The proofing room volume was meshed using more than 2,900,000 tetrahedral cells.

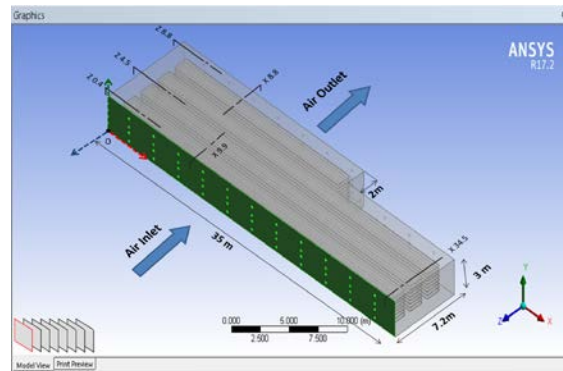


Fig.1. large storing room configuration

Meshing independency study

The mesh dependency was examined by solving the flow field for three mesh configurations made of 2100000, 2900000 and 3600000 cells respectively. The simulation results showed that up to 4 % difference in relative humidity existed between the coarser and finer mesh, and less than 0.29 % difference existed between the two finer meshes, so that the mesh size of 2900000 was selected for this simulation.

temperature and relative humidity. Results of the simulation for a case study of a large fermentation room were compared to the experimental result which showed fair agreement. Figures (2) and (3) show the plotting of measured and simulated relative humidity and temperature respectively in a large proofing room. Small variation in values between simulations and experiments are recorded for air temperature and relative humidity, but their maxi-

imum difference is under 2%. The measured outdoor air temperature and relative humidity at the time of experiment is recorded as $37\pm 1^\circ\text{C}$ and $57\pm 3\%$ respectively.

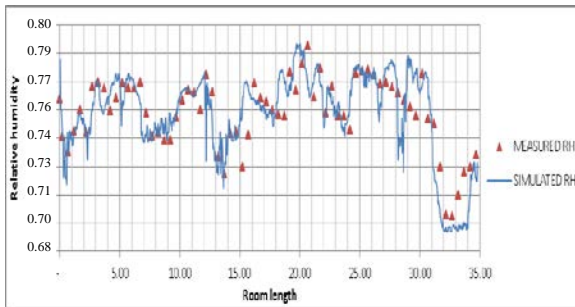


Fig.2. Measured and simulated relative humidity at z4.5 y1.5

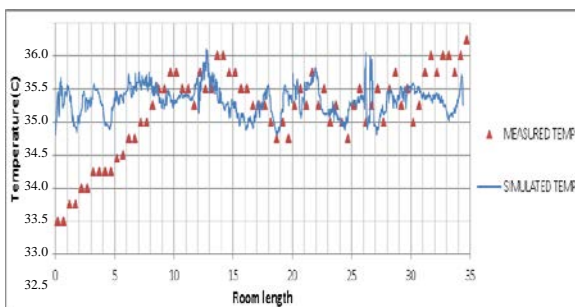


Fig.3. Measured and simulated Temperature at z4.5 y1.5

RESULTS AND DISCUSSIONS

In this paper, numerical CFD simulation has been performed to study the air flow patterns, temperature distribution and relative humidity distribution in a large refrigeration store onboard marine ships. Different model configurations have been introduced representing the different inlet air speeds and flow rates. This comparative study includes the analysis of different inlet air speeds in order to select the best design configuration of large refrigeration stores among these studied cases.

Figure (4) shows relative humidity distribution in a vertical plane z0.4m (the midsection of the store) at height y1.5m for different inlet air flow rate model configurations. The relative humidity distribution shows a significant relative humidity change in front of inlet ports due to higher velocity magnitude.

Figure (5) shows relative humidity distribution in a vertical plane z4.5m at height y2.5m for different model configurations. Inlet air flow rate configurations from $3.8\text{ m}^3/\text{s}$ to $8.2\text{ m}^3/\text{s}$ show significant increase in relative humidity. Relative humidity ranges from $3.8\text{ m}^3/\text{s}$ to $5.2\text{ m}^3/\text{s}$ related to inlet speeds 2.5 m/s to 3.5 m/s respectively can be considered optimum to avoid high air speeds and product dehydration. Also, this air speed range is better for energy saving.

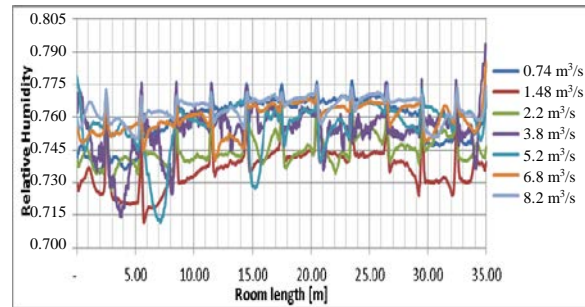


Fig.4. Measured and simulated relative humidity at z0.4 y1.5 at various air flow rates models.

Figure (5) shows relative humidity distribution in a vertical plane z4.5m at height y2.5m for different model configurations. Inlet air flow rate configurations from $3.8\text{ m}^3/\text{s}$ to $8.2\text{ m}^3/\text{s}$ show significant increase in relative humidity. Relative humidity range from $3.8\text{ m}^3/\text{s}$ to $5.2\text{ m}^3/\text{s}$ related to inlet speeds 2.5 m/s to 3.5 m/s respectively can be considered optimum to avoid high air speeds and product dehydration. Also this air speed range is better for energy saving.

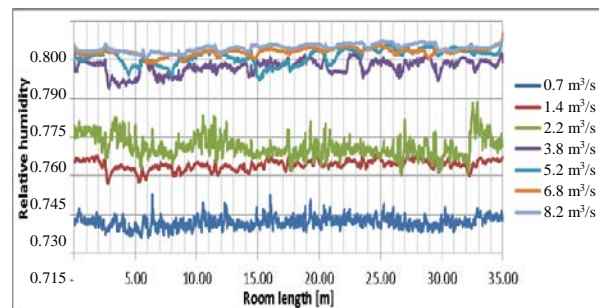


Fig.5. Relative humidity distribution at z4.5m y2.5m at various inlet air flow rates

Figure (6) shows temperature distribution in a vertical plane z4.5m (the midsection of the store) at height y1.5m for different models. The figure shows that the temperature range inside the fermentation room is 0.6°C for all studied configurations. Temperature field distribution and values recorded inside the large store can be considered acceptable for all model configurations.

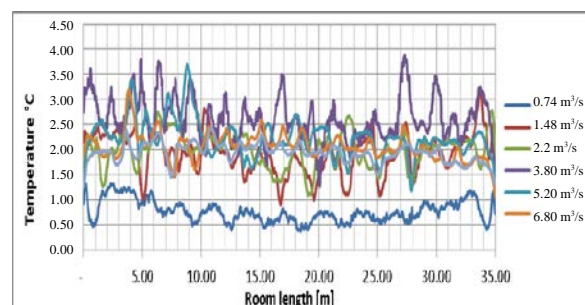


Fig.6. Temperature distribution at z4.5m and height y1.5m at various inlet air speeds

Figures (7) and (8) show relative humidity contours in a horizontal plane y1.6m for 1.0 m/s and 5.5 m/s models.

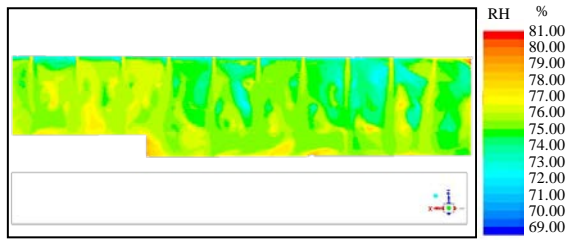


Fig.7. Relative humidity contours at y1.6m in 3.8 m³/s air distribution model

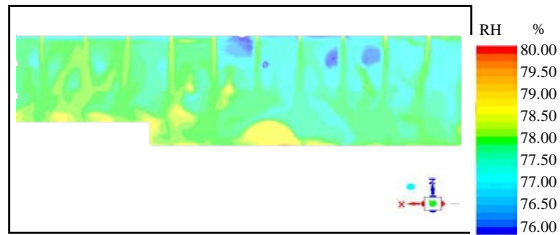


Fig.8. Relative humidity contours at y1.6m in 8.2 m³/s air distribution model

Figures (9) and (10) show air velocity magnitude contours in a horizontal plane y1.6m for 3.8 m³/s and 8.2 m³/s models respectively.



Fig. 9. Air velocity magnitude contours at y1.6m in 3.8 m³/s air distribution model

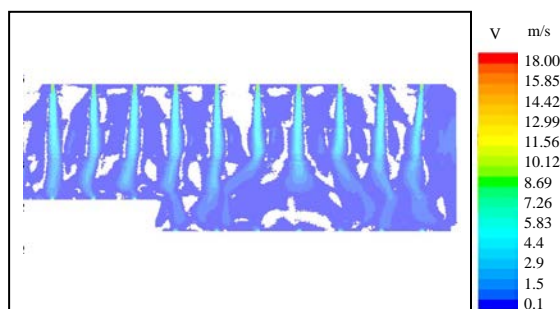


Fig.10. Air velocity magnitude contours at y1.6m in 8.2 m³/s air distribution model

Figures 11(a) and 11(b) show relative humidity distribution in two transverse planes x34.5m and x9.9m at height y2.5m and 1.6m respectively.

Regions of abrupt changes and continuous fluctuations are considered as suspicious areas which are optimum for sensor locations inside the large refrigeration store.

Figures (13) and (14) show relative humidity distribution in two vertical planes z8.8m and z0.4m at

height y2.5m.

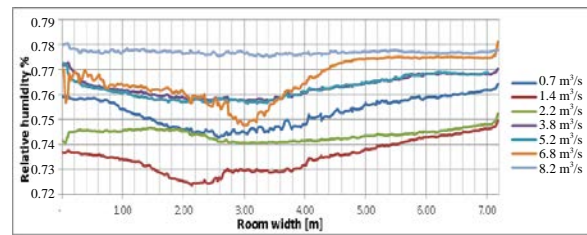


Fig.11.a Relative humidity distribution at x34.5m and y2.5m at various inlet air flow rates

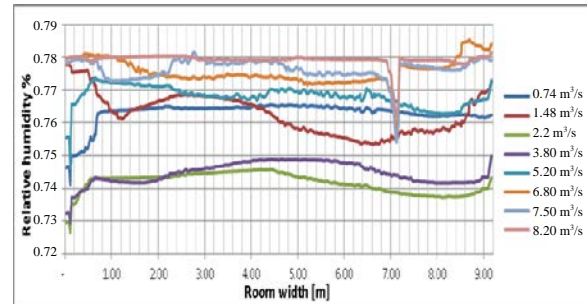


Fig.11.b Relative humidity distribution at x9.9m and y1.6m at various inlet air flow rates

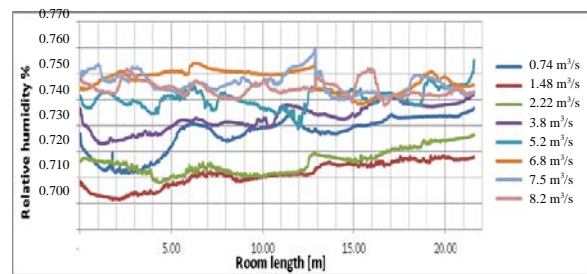


Fig. 13. Relative humidity distribution at z8.8m and y2.5m at various inlet air flow rates

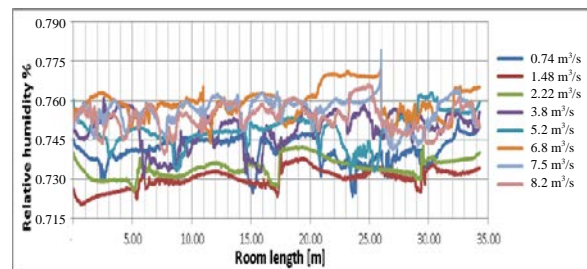


Fig. 14. Relative humidity distribution at z0.4m and y2.5m at various inlet air flow rates

From Figures (11) to (14) temperature and relative humidity sensors should be located at the following position coordinates: A (34.5m, 2.5m, 3m), B (9.9m, 1.6m, 7m), C (3m, 2.5m, 8.8m) and D (32m, 2.5m, 0.4m). Majority of sensors are located on height 2.5m at which fluctuations and abrupt changes were noticed in values of temperature and relative humidity.

CONCLUSIONS

In this paper, a set of steady-state simple models to simulate air flow in large refrigeration

stores onboard marine ships are presented. These simple models can be used to study any typical large refrigeration store by simulating the temperature distribution, relative humidity distribution and air velocity magnitude according to different inlet air speed and flow rates.

- The relative humidity and temperature field distribution and values recorded inside the large refrigeration store model can be considered acceptable.
- For optimum special stores air quality, inlet air speed should range between 2.5m/s to 3.5m/s which relates to inlet air flow rates from 3.8 m³/s to 5.2 m³/s. This speed range is suitable for preventing mold build up on store walls and avoiding product dehydration.
- Inlet air speed range from 2.5m/s to 3.5m/s is better in energy saving.
- For optimum special stores air quality in large refrigeration stores, inlet volume flow rate per cubic meters of the store volume should be in range between 3.94 L/s/m³ to 5.38 L/s/m³.
- Contours of air velocity magnitude inside room show acceptable air velocity magnitude in most room areas.
- Recommended air flow rate range with 20% fresh air admits acceptable air change inside special refrigeration stores.
- Optimum temperature and relative humidity sensor locations could be selected according to simulation results.

NOMENCLATURE

ρ	Density of air
P	Air pressure
u	Molecular viscosity
u_t	Turbulent viscosity
T	Air Temperature
τ	Viscous Stress
p	Thermodynamic pressure
M	Mean Value
k_t	Turbulent thermal conductivity
K	Molecular thermal conductivity
u, v, w	Velocities in the directions of x, y, z

REFERENCES

- Bamodu, O., Xia, L. and Tang, L., "A numerical Simulation of Air Distribution in an Office Room Ventilated by 4-Way Cassette Air-conditioner," Energy Procedia, vol.105, p. 2506-2511 (2017).
- Cengel, Y.A. and Ghajar, A.J., "Refrigeration and Freezing of Foods, Chapter 17. In: Heat and Mass Transfer: Fundamentals and Applications," McGraw-Hill, 2013. HVAC system simulation. Automation in Construction, vol.19, Iss.2, p. 93-99 (2013).
- Han, M.G., May, R., Zhang, X.X., Wang, X.R., Pan, S., Yan, D., ..., Xu, L.G., "A Review of Reinforcement Learning Methodologies for Controlling Occupant Comfort in Buildings," Sustainable Cities and Society, vol.51, 101748 (2019).
- Homod, R.Z., "Review on the HVAC System Modeling Types and the Shortcomings of Their Application," Journal of Energy, Article ID 768632 (2013).
- Homod, R.Z., Salleh, K., Sahari, K., Mohamed, H. A F, Nagi, F., "Hybrid PID-cascade Control for HVAC System," International Journal of Systems Control, vol.1, Iss.4, p. 170-175 (2010).
- Knabe, G. and Le, H.T., "Building Simulation by Application of a HVAC System Considering the Thermal and Moisture Behaviors of the Perimeter Walls," IBPSA Building Simulation Proceedings, p. 965-972 (2011).
- Kono, Y., et al., "Multiscale modeling of in-room temperature distribution with human occupancy data: a practical case study," Journal Oerence of IBPSA, Chambery, France (2013).
- Mahu, R., Popescu, F. and Ion, I.V., "CFD Modeling Approach for HVAC Systems Analysis," Chemical Bulletin of Politehnica University of Timisoara, p. 69-73 (2012).
- Pascual, J.A.F., et al., "Heat Ventilation and Air Conditioning Modeling for Model Based Fault Detection and Diagnosis," in Proceedings of 13th Conference of IBPSA, Chambery, France (2013).
- Popovici, C.G., "HVAC system functionality simulation using ANSYS-Fluent," Energy Procedia, vol. 112, p. 360-365 (2017).
- Wang, W., et al., "Multi-zone Outdoor Air Coordination Through Wi-Fi Probe-based Occupancy Sensing," Energy and Buildings, vol. 159, p. 495-507 (2018).